

CHEMICAL ABUNDANCES OF MEMBER STARS IN THE OPEN CLUSTER NGC 2632 (PRAESEPE)

X. L. YANG^{1,2}, Y. Q. CHEN¹, AND G. ZHAO¹¹ Key Laboratory of Optical Astronomy, National Astronomical Observatories, Chinese Academy of Sciences,
20A Datun Road, Chaoyang District, 100012 Beijing, China² University of Chinese Academy of Sciences, 19A Yuquan Road, 100049 Beijing, China*Received 2015 July 29; accepted 2015 September 24; published 2015 October 26*

ABSTRACT

Based on high-resolution, high signal-to-noise ratio spectra, we present abundances of 17 elements (Fe, O, Na, Mg, Al, Si, Ca, Sc, Ti, V, Cr, Co, Ni, Y, Zr, Ba, La) for six stars (one Am star, one F dwarf star, and four GK giant stars) and radial velocities for 18 proper-motion selected member stars in the open cluster NGC 2632. In the Am star, s-process elements Y and Ba are clearly overabundant, which may be considered as an indicator of a peculiar Am star. The average $[\text{Fe}/\text{H}]$ is 0.16 ± 0.06 from four GK giant member stars, which is similar to that of solar-type stars in the literature. As compared with dwarf stars, significant overabundances are found for Na, Mg, and Ba elements in our giant stars, which can be explained by the evolutionary effect. We also detect a star-to-star scatter of $[\text{Na}/\text{Fe}]$ ratios among four giants which locate approximately at the same position in the CMD. Finally, we perform an analysis on the possible connection between the abundance and spatial structure of NGC 2632, but we find no inhomogeneous abundance among different clumps of stars in this cluster based on our limited sample.

Key words: Galaxy: disk – open clusters and associations: individual (NGC 2632) – stars: abundances

1. INTRODUCTION

Open clusters (OCs) provide important information in the study of stellar evolution, dynamical evolution, and chemistry of the Galactic thin disk at various Galactic coordinates and at different epochs. Stars in OCs are believed to form from the same protocluster cloud, and thus they have the same age, distance, and chemical composition. Therefore, their properties such as distance, reddening, and age can be determined with smaller uncertainties than field stars. Spectral analysis of member stars in a given OC is important to study the stellar evolution and to trace the chemical evolution of the Galactic disk by deriving precise abundances for many elements.

Among more than 2000 OCs in the Galaxy (Dias et al. 2002), NGC 2632 (also called Praesepe or M44) is an interesting nearby OC. First, it has been suggested to be formed from two merging clusters according to Holland et al. (2000), where the contour and density plots indicate the existence of a subcluster with a mass of $\sim 30 M_{\odot}$ and the anomalous X-ray results suggested a different age between the main cluster and the subcluster. This suggestion that NGC 2632 may have been formed by two merged clusters of different ages was further confirmed by Franciosini et al. (2003) based on new X-ray data. Recently, a study of the internal structure and kinematics of NGC 2632 by Vereshchagin & Chupina (2013) shows that the cluster consists of a homogeneous core and a non-uniform corona that may contain three or four real clumps. It is interesting to probe whether NGC 2632 will also show inhomogeneous features in abundance. Second, NGC 2632 consists of various types of stars at different evolutionary stages, including delta Scuti stars (Breger et al. 2012), blue straggler stars (Fossati et al. 2010), Am stars, normal A stars, FGK dwarfs, M dwarfs (Kafka & Honeycutt 2006), white dwarfs (Casewell et al. 2009), brown dwarfs (Boudreault et al. 2010), G subgiants, and K giants. Spectral analysis of these stars could provide crucial constraints on the stellar evolution theory in the OC environment.

NGC 2632 is a young OC with an age of 0.7 Gyr located at about 8.62 kpc from the Galactic center and 85 pc above the

disk plane (Salaris et al. 2004). High-resolution and high signal-to-noise ratio (S/N) spectral analyses of member stars in NGC 2632 have been carried out in several works. However, the metallicity of this cluster provided in these works covers a wide range from +0.04 to +0.27. Friel & Boesgaard (1992) obtained $[\text{Fe}/\text{H}] = +0.04 \pm 0.04$ based on six F dwarfs, while Pace et al. (2008) derived a supersolar metallicity of $+0.27 \pm 0.10$ from seven solar-type stars. Moreover, different metallicities are also reported for solar-type stars in different works. For example, Boesgaard et al. (2013) derived $[\text{Fe}/\text{H}] = +0.12 \pm 0.04$ from 11 solar-type stars, which is 0.15 dex lower than that of Pace et al. (2008). Based on three red giant stars in NGC 2632, Carrera & Pancino (2011) obtained $[\text{Fe}/\text{H}] = +0.16 \pm 0.05$, which supports the result of Boesgaard et al. (2013). For other elements, abundance differences also exist among member stars of NGC 2632 in previous works. A significantly underabundant $[\text{O}/\text{Fe}]$ of -0.42 ± 0.08 was reported by Pace et al. (2008) for seven solar-type stars, while Boesgaard et al. (2013) obtained $[\text{O}/\text{Fe}] = -0.146 \pm 0.089$ based on 11 solar-type stars. According to Carrera & Pancino (2011), $[\text{Y}/\text{Fe}] = -0.11 \pm 0.01$ was slightly lower than solar value based on the three giants, but the solar $[\text{Y}/\text{Fe}]$ ratio was found by Boesgaard et al. (2013). Obviously, some of these differences in metallicity and abundance ratios for NGC 2632 among different works come from inconsistent abundance analyses (e.g., adopting different stellar parameters and atomic data of various lines, etc.). However, it is also possible that abundance differences among cluster member stars really exist. For example, we may suspect that at least some of these discrepancies come from the study of different spectral types of member stars. Member stars in different clumps of non-uniform corona as shown in Vereshchagin & Chupina (2013) are also possible to show discrepancies in abundance.

In this work, we observed 18 stars with different spectral types (Am dwarfs, normal A stars, F dwarfs, G subgiant, and GK giants) in the NGC 2632 field. The main goals of this study are threefold. First, the abundance pattern of the OC NGC 2632 can be studied in a better way with more member stars. Second,

we aim to discuss the abundance differences among different types of stars. Finally, we attempt to perform a careful analysis on the possible connection between the abundance and spatial structure of NGC 2632 for the first time.

2. OBSERVATIONS AND DATA REDUCTION

The target stars were selected from the WEBDA³ database using the following criteria. The membership probabilities of proper motion (PM) are larger than 70%. The V magnitudes are brighter than 9.5 mag, which enables us to obtain high-resolution and high signal-to-noise spectra with the 2.16 m telescope at Xinglong station of NAOC. Finally, we prefer to select stars that have not been previously studied with high-resolution spectroscopy but keep a few stars in common for comparison. The final sample consists of 18 stars.

Observations were carried out with a high-resolution spectrograph attached to the 2.16 m telescope of the National Astronomical Observatories (Xinglong, China) during four observation runs, 2012 February and April and 2013 March and November. The spectral resolution is about 50,000 and the wavelength coverage is from 4000 to 9000 Å, but only the 5000–7800 Å region was finally employed in order to obtain reliable normalization in the blue end and to avoid the interference fringes in the red. The S/N of the spectra ranges from 90 to 170 pixel⁻¹ at 6000 Å.

The spectra were reduced with IDL programs for order identification, background subtraction, flat-field correction, wavelength calibration, and spectrum extraction. Then, we used the MIDAS programs for radial velocity (RV) measurement, continuum normalization, and equivalent width (EW) measurements (see Chen et al. 2000 for details). Table 1 presents star names, KW numbers, coordinates, magnitudes, spectral types, radial velocities from our spectra and from the literature, PMs, and observational information for 18 stars in our selected sample.

3. MEMBER STARS, SPECTRAL TYPES, AND THE DISTRIBUTIONS IN SPACE AND THE COLOR–MAGNITUDE DIAGRAM

3.1. Member Stars

According to Dias et al. (2002, catalog updated in 2014), the OC NGC 2632 has an RV of 34.76 km s⁻¹ and a PM in $\mu_\alpha \cos \delta$ of $-35.58 \text{ mas yr}^{-1}$ and in μ_δ of $-12.90 \text{ mas yr}^{-1}$. The PM distribution from the PPMXL data given by Wang et al. (2014) for this cluster is $\mu_\alpha \cos \delta \approx -36.5 \text{ mas yr}^{-1}$ and $\mu_\delta \approx -13.5 \text{ mas yr}^{-1}$. Based on these values, we inspect our target stars. First, we find that HD 73712 has a slightly large deviation in PM. It is worth mentioning that HD 73712 is a spectroscopic binary and its RV varies with time. The RV measured from our spectra is just a value at the observation time, which is affected by its companion and cannot be used to determine its membership. However, according to Pourbaix et al. (2004), the RV value at amplitude = 0 in the RV curve, which is not affected by its companion, is 34.40 km s⁻¹. This indicates that the intrinsic RV for HD 73712 is actually consistent with that of the OC. Thus it could be a member star of NGC 2632. Comparing the RV values from our spectra with those from the literature, three stars, HD 73174, HD 73618, and HD 73709, show inconsistent values. Note that HD 73174 and HD 73709

are suspected to be a spectroscopic binary according to Pourbaix et al. (2004) and HD 73618 is a double or multiple star as suggested by Eggleton & Tokovinin (2008), which may cause variations in RV. In addition, the three stars have consistent PMs with NGC 2632, thus we suggest that they could be member stars of this cluster and keep them in our sample in the following analysis. The remaining targets are cluster members in both PM and RV.

3.2. Spectral Types of Member Stars

Among the 18 member stars, 6 are A type stars. Most of them have large rotational velocities and their spectra contain very few lines, which makes it impossible to carry out an abundance analysis. Fortunately, we have an Am star, HD 73174, which has low rotational velocity and contains enough narrow lines for abundance analysis. We have seven F-type stars in our member list, but only one star, HD 73081, shows low rotational velocity. The most exceptional case is the only subgiant, HD 72779, which has almost no metal lines in its spectra. This subgiant is a member star in both PM and RV. According to Uesugi & Fukuda (1970), the rotational velocity of HD 72779 is 95 km s⁻¹. This is on the high side since the rotational velocity spins down significantly as it evolves from the main-sequence to subgiant stage. The high rotational velocity makes it impossible to perform further abundance analysis. The remaining four stars are GK type giants. In total, we have six stars for abundance analysis.

3.3. The Distributions of our Member Stars in Space and the Color–Magnitude Diagram

Figure 1 shows the Galactic locations of the 18 member stars. Six member stars with enough lines in their spectra for abundance measurements are indicated by filled circles. The small dots are possible member stars of NGC 2632 with a PM probability larger than 50% in Adams et al. (2002). The cross is the center of the cluster and the solid line is the core region with a diameter of 65 arcmin as described in Vereshchagin & Chupina (2013). We also show the location of the central region with a radius of 3 pc (corresponds to 27.5 arcmin) in Holland et al. (2000) with the dashed line. We can see that 14 of our member stars are within the core region and only 4 member stars are located in the part of the non-uniform corona. The color–magnitude diagram for the 18 member stars is shown in Figure 2. It shows that all target stars fit the evolutionary track well.

4. ABUNDANCE ANALYSIS FOR SIX MEMBER STARS IN NGC 2632

4.1. Stellar Atmospheric Parameters

For the six member stars (HD 73081, HD 73174, HD 73598, HD 73665, HD 73710, and HD 73974) with enough narrow lines for an abundance analysis, we compile the $(B - V)$, $(V - K)$, and $(b - y)$ color indices from the SIMBAD⁴ website and obtain the dereddened $(B - V)_0$, $(V - K)_0$, and $(b - y)_0$ assuming a reddening value of $E(B - V) = 0.027 \pm 0.004$ (Taylor 2006). Then we derive the effective temperatures, T_{eff} , from the three sets of photometric data using the empirical calibration relations of Alonso et al. (1996, 1999, 2001). In the

³ <http://www.univie.ac.at/webda/>

⁴ <http://simbad.u-strasbg.fr/simbad/>

Table 1
Target Stars Observed with HRS in the Field of NGC 2632

Star	KW	R.A. (2000)	DECL. (2000)	V (mag)	spType	RV (This)	RV (Ref.)	PMra	PMdec	Obs. Date	Remarks
HD 72779	1133	08:35:19.4	+19:35:24	6.58	G0	37.81	34.90	-35.31	-11.83	12 Feb 03	...
HD 73081	16	08:37:02.0	+19:36:17	9.19	F6	36.50	33.75	-35.50	-12.10	13 Nov 19	...
HD 73161	38	08:37:33.8	+20:00:49	8.71	F0	30.76	36.34	-34.80	-12.90	13 Mar 25	...
HD 73174	40	08:37:37.0	+19:43:59	7.76	Am	43.75	35.64 ^b	-34.40	-13.40	12 Apr 04	Spectroscopic binary ^b
HD 73397	124	08:38:47.0	+19:30:03	9.06	F4	36.94	36.20 ^a	-34.20	-10.10	13 Nov 17	...
HD 73598	212	08:39:50.7	+19:32:27	6.60	K0	35.42	34.97	-34.08	-13.07	13 Mar 23	Double or multiple star ^c
HD 73616	226	08:39:58.4	+20:09:29	8.93	F2	32.09	31.00	-37.20	-13.50	13 Mar 25	...
HD 73618	224	08:39:56.5	+19:33:11	7.30	Am	29.56	40.00	-36.00	-11.60	13 Nov 16	Double or multiple star ^c
HD 73665	253	08:40:06.4	+20:00:28	6.39	G8	33.44	33.88	-36.17	-11.26	12 Feb 06	...
HD 73709	279	08:40:20.8	+19:41:12	7.68	F2	64.68	36.51 ^b	-36.90	-11.90	13 Mar 27	Spectroscopic binary ^b
HD 73710	283	08:40:22.1	+19:40:12	6.39	G9	34.15	34.32	-36.04	-12.90	12 Feb 06	...
HD 73711	276	08:40:18.1	+19:31:55	7.51	F0	34.46	39.00	-32.80	-11.30	13 Mar 28	...
HD 73712	287	08:40:20.2	+19:20:56	6.78	A9	31.03	34.40 ^b	-38.48	-8.52	13 Mar 27	Spectroscopic binary ^b
HD 73731	300	08:40:26.9	+19:32:39	6.29	A5	25.74	29.90 ^b	-35.60	-12.98	12 Feb 04	Spectroscopic binary ^b
HD 73785	328	08:40:43.2	+19:43:09	6.84	A9	32.86	34.60	-35.06	-11.51	13 Mar 23	...
HD 73854	370	08:41:10.7	+19:49:46	9.03	F5	34.60	33.00	-38.10	-13.20	13 Mar 28	...
HD 73872	379	08:41:13.8	+19:55:19	8.34	A5	32.43	31.00	-37.10	-13.20	13 Mar 24	Variable Star of delta Sct type ^d
HD 73974	428	08:41:50.0	+19:52:27	6.92	K0	28.59	33.62 ^b	-34.98	-14.80	12 Apr 03	Spectroscopic binary ^b

Notes. The data information is taken from SIMBAD.

^a Dickens et al. (1968).

^b Pourbaix et al. (2004).

^c Eggleton & Tokovinin (2008).

^d Breger et al. (2012).

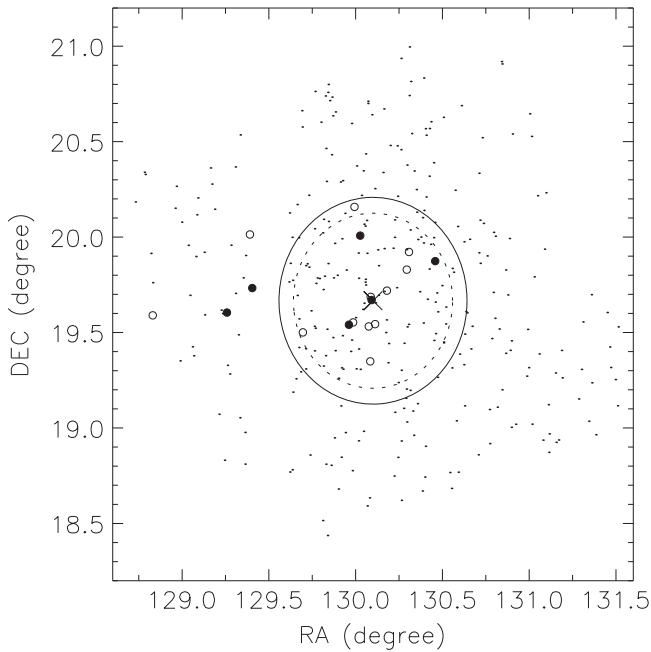


Figure 1. Galactic locations of 18 stars (open and filled circles) in this work. Different symbols correspond to specific stars: possible member stars with a proper motion probability larger than 50% in Adams et al. (2002); dots; six stars with enough lines for abundance measurements (filled circles); the cluster center (cross); the core region with a diameter of 65 arcmin described in Vereshchagin & Chupina (2013; solid line); and the central region with a radius of 3 pc described in Holland et al. (2000; dashed line).

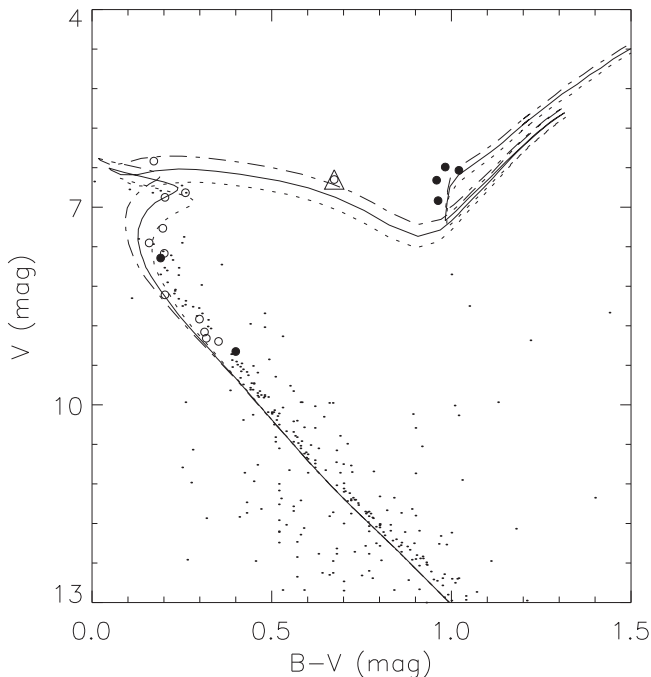


Figure 2. Color-magnitude diagram of NGC 2632. The symbols are the same as in Figure 1. The subgiant HD 72779 is marked with an additional triangle. The solid line, dotted line, and dash-dotted line represent the isochrones (Girardi et al. 2000) for $\log(\text{Age}) = 8.80, 8.85,$ and $8.75,$ respectively.

case of HD 73598, we have no K magnitude, so we only give the T_{eff} from $(B - V)_0$ and $(b - y)_0$ photometric data. Table 2 shows the three sets of T_{eff} for the six stars, and they show very good consistence. Given that the narrowband photometric data

($uvby$) have higher precision for parameter determination, T_{eff} from $(b - y)_0$ are adopted in the following abundance measurements.

The surface gravity ($\log g$) is determined based on the *Hipparcos* parallax using the following formulae:

$$\log g = \log g_{\odot} + \log \left(\frac{M}{M_{\odot}} \right) + 4 \log \left(\frac{T_{\text{eff}}}{T_{\text{eff},\odot}} \right) + 0.4(M_{\text{bol}} - M_{\text{bol},\odot}) \quad (1)$$

$$M_{\text{bol}} = V + BC + 5 \log \pi + 5 - A_v \quad (2)$$

where M is the stellar mass, which is obtained from Yale-Yonsei stellar evolution tracks (Yi et al. 2003), and M_{bol} , V , BC , π , and A_v represent the bolometric magnitude, apparent magnitude, bolometric correction, parallax, and interstellar extinction, respectively. The bolometric corrections are derived with estimated effective temperatures and metallicities (Alonso et al. 1996, 1999) and interstellar extinction is adopted using $A_v = 3.1E(B - V)$. We also determine the spectroscopic $\log g$ by forcing Fe I and Fe II lines to give the same iron abundance. Comparing these spectroscopic gravities with values determined from *Hipparcos* parallaxes, we find that all stars follow the one-to-one relation well. For the F-type star, HD 73081, the *Hipparcos* parallax is not available, and thus we adopt the spectroscopic value, although the value 4.43 for the F dwarf star is slightly high.

The microturbulence, ε_t , is determined by requiring a zero slope relation between iron abundance and EW. We choose a set of Fe I lines with accurate oscillator strengths, similar excitation potentials, and a large range of EWs ($10 \text{ m}\text{\AA} < \text{EW} < 110 \text{ m}\text{\AA}$) for the microturbulence determination. The initial metallicity for our stars is set to $[\text{Fe}/\text{H}] = 0.2 \text{ dex}$, a value between 0.12 dex from Boesgaard et al. (2013) and 0.27 dex from Pace et al. (2008). The spectroscopic metallicity from our analysis is adopted when available. Given that the atmospheric parameters were not determined independently, we adopt the final results by iterating the whole processes of determining the atmospheric parameters T_{eff} , $\log g$, $[\text{Fe}/\text{H}]$, and ε_t several times until they are consistent. The final adopted stellar parameters for our target stars are presented in Table 2. The uncertainties are about 70 K in temperature, 0.1 dex in gravity and metallicity, and 0.3 km s^{-1} in microturbulence.

4.2. Line List, Atomic Data, EW Measurements, and Abundance Determinations

Most of our atomic line data are taken from Liu et al. (2012), Tsantaki et al. (2013), and Ramírez et al. (2014). Since the atomic data are compiled from different references, the results might be affected systematically. Therefore, we took a 10 s exposure of the moon to be used as a surrogate for the solar spectrum. In this work, the adopted atomic line data are corrected to obtain solar abundances based on our solar spectrum, and our final results are the stars' differential values relative to the Sun.

We have calculated the EWs using three methods: direct integration and Gaussian and Voigt function fitting. For weak and intermediate-strength lines, we fitted the line profiles with a Gaussian function, whereas strong lines were fitted with a

Table 2
Stellar Parameters for Six Stars

Star	Derived T_{eff}			Derived $\log g$		Adopted Parameters			
	T_{eff}^{B-V}	T_{eff}^{V-K}	T_{eff}^{b-y}	$\log g^{\text{phot}}$	$\log g^{\text{spec}}$	T_{eff}	$\log g$	[Fe/H]	ε_t
HD 73081	6865	6884	6873	...	4.43	6873	4.43	0.06	1.57
HD 73174	8104	8087	8121	4.1	4.03	8121	4.03	0.37	3.00
HD 73598	4953	...	5002	2.8	2.81	5002	2.81	0.16	1.54
HD 73665	4942	5034	4964	2.8	2.65	4964	2.65	0.20	1.64
HD 73710	4853	4990	4859	2.7	2.60	4859	2.60	0.13	1.64
HD 73974	4978	4951	4954	2.8	2.82	4954	2.82	0.13	1.54

Voigt function. If unblended lines are well separated from nearby lines, direct integration was adopted. We discarded strong lines with $\text{EW} > 110 \text{ m\AA}$ for Fe I lines, $\text{EW} > 200 \text{ m\AA}$ for Ba II lines, and $\text{EW} > 150 \text{ m\AA}$ for other lines.

Based on the plane-parallel, homogeneous, and local thermodynamic equilibrium (LTE) model (Kurucz 1993; Castelli & Kurucz 2004), we determine the chemical abundances using the ABONTEST8 program supplied by Dr. P. Magain, which calculates the theoretical EWs from model and matches them with observed values. Several broadening mechanisms are taken into account, including natural broadening, thermal broadening, van der Waals damping broadening, and microturbulent broadening. We have derived the $[X/\text{Fe}]$ ratios of 16 elements (O, Na, Mg, Al, Si, Ca, Sc, Ti, V, Cr, Co, Ni, Y, Zr, Ba, La). In particular, the O abundance is derived from O I triplet lines. For four giant stars, $[\text{O}/\text{Fe}]$ ratios have been corrected for non-LTE effects through the calculations of Takeda (2003).

4.3. Error Analysis

We estimate the uncertainties of the abundances by taking into account two error sources. One is the internal (random) uncertainty, including uncertainties related to the measurement of EWs and to the atomic data ($\log gf$). Errors in EW measurements come from the choice of the continuum, the mixture of spectral lines, and the S/N. Errors in $\log gf$ values are not significant, since they should be almost eliminated when subtracting the solar abundances from the stellar ones. So we finally only use $\sigma_{\text{EW}}/\sqrt{N_{\text{lines}}}$ as the internal error.

The other error source is the uncertainties from the stellar parameters (T_{eff} , $\log g$, $[\text{Fe}/\text{H}]$, and ε_t). To estimate the impact of the stellar parameter choice on the derived abundances, we alter the value of one parameter and recalculate the abundances with the same procedure described in the previous section, while all the other parameters are kept unchanged. Table 3 presents the effects on the derived abundances resulting from the increases by 70 K in effective temperature, 0.1 dex in gravity, 0.1 dex in metallicity, and 0.3 km s^{-1} in microturbulence. Finally, we add quadratically all the individual errors as the total error.

5. RESULTS AND DISCUSSION

Based on high-resolution spectra and standard LTE analysis, we have derived abundance ratios of the light elements (Na, Al), α elements (O, Mg, Si, Ca, Ti), iron-peak elements (Sc, V, Cr, Fe, Co, Ni), light s-process elements (Y, Zr), and heavy s-process elements (Ba, La). Table 4 gives the $[\text{Fe}/\text{H}]$ and $[X/\text{Fe}]$ values of six stars. The metallicities vary from 0.06 to 0.37 dex among the six stars. In particular, HD 73174 is an Am star, and its $[\text{Fe}/\text{H}]$ (0.37 dex) is higher than other stars by

Table 3
Abundance Errors for HD 73665

Element	$\frac{\sigma_{\text{EW}}}{\sqrt{N}}$	ΔT_{eff} (+70 K)	$\Delta \log g$ (+0.1)	$\Delta [\text{Fe}/\text{H}]$ (+0.1)	$\Delta \varepsilon_t$ (+0.3)	σ_{tot}
$\Delta[\text{Fe I}/\text{H}]$	0.01	0.04	0.01	0.02	-0.06	0.076
$\Delta[\text{Fe II}/\text{H}]$	0.03	-0.05	0.06	0.04	-0.06	0.110
$\Delta[\text{O}/\text{Fe}]$	0.04	-0.11	0.01	-0.04	0.03	0.128
$\Delta[\text{Na}/\text{Fe}]$	0.03	0.06	-0.04	-0.02	0.00	0.081
$\Delta[\text{Mg}/\text{Fe}]$	0.03	0.02	-0.06	-0.04	0.02	0.083
$\Delta[\text{Al}/\text{Fe}]$	0.03	0.04	-0.04	-0.03	0.03	0.077
$\Delta[\text{Si}/\text{Fe}]$	0.02	-0.01	-0.01	-0.01	0.02	0.033
$\Delta[\text{Ca}/\text{Fe}]$	0.03	0.05	-0.04	-0.03	-0.04	0.087
$\Delta[\text{Sc}/\text{Fe}]$	0.04	0.00	0.01	0.00	-0.03	0.051
$\Delta[\text{Ti}/\text{Fe}]$	0.03	0.06	-0.03	-0.03	0.02	0.082
$\Delta[\text{V}/\text{Fe}]$	0.06	0.05	-0.03	-0.04	-0.02	0.095
$\Delta[\text{Cr}/\text{Fe}]$	0.06	0.02	-0.03	-0.03	0.00	0.076
$\Delta[\text{Co}/\text{Fe}]$	0.03	0.06	-0.01	-0.01	0.02	0.071
$\Delta[\text{Ni}/\text{Fe}]$	0.02	0.03	-0.01	-0.01	-0.01	0.040
$\Delta[\text{Y}/\text{Fe}]$	0.01	0.00	0.02	0.01	-0.01	0.026
$\Delta[\text{Zr}/\text{Fe}]$	0.04	0.09	-0.03	-0.03	0.05	0.122
$\Delta[\text{Ba}/\text{Fe}]$	0.02	0.02	0.00	0.02	-0.08	0.087
$\Delta[\text{La}/\text{Fe}]$	0.05	0.01	0.01	0.01	0.04	0.066

0.2–0.3 dex. Moreover, the only F dwarf, HD 73081, has the lowest metallicity of 0.06 dex. For the four giant targets, we obtain the average $[\text{Fe}/\text{H}] = 0.16 \pm 0.06$, which is exactly the same as that of Carrera & Pancino (2011) who derived $[\text{Fe}/\text{H}] = 0.16 \pm 0.05$ from three of them.

5.1. Abundance of the Am Dwarf

The Am character of HD 73174 was first found by Bidelman (1956) based on spectrograms. Later, high-resolution spectral analyses of HD 73174 were carried out by different authors. Hui-Bon-Hoa & Alecian (1998) derived detailed abundances for Mg, Ca, Sc, Cr, Fe, and Ni elements; Burkhart & Coupry (1998) determined abundances for Li, Al, Si, S, Fe, Ni, and Eu elements; and Fossati et al. (2007) gave abundances for 32 elements.

Our $[\text{Fe}/\text{H}]$ value for HD 73174 is 0.37 dex, which is consistent with the results of Hui-Bon-Hoa & Alecian (1998) and Burkhart & Coupry (1998). However, Fossati et al. (2007) gave a much higher $[\text{Fe}/\text{H}]$ value of 0.71 dex. Note that HD 73174 is a spectroscopic binary according to several works (e.g., Debernardi et al. 2000; Pourbaix et al. 2004). The RV of HD 73174 determined by Fossati et al. (2007) is 2.9 km s^{-1} , while the value is 43.75 km s^{-1} from our spectra. This indicates that HD 73174 was in different states with its component at different observation times. We are not sure whether the component will impact the spectra, or at least some metallic

Table 4
Metallicities and Abundance Ratios of Six Member Stars of NGC 2632

Ratio	HD 73174	HD 73081	HD 73665	HD 73710	HD 73598	HD 73974	Mean _{Giants}	C11 ^a	B13 ^b
	Am	F6 IV	G8 III	G9 III	K0 III	K0 III	Four Giants	Three Giants	11 Solar Type Stars
[Fe/H]	0.37	0.06	0.20	0.13	0.16	0.13	0.16 ± 0.06	0.16 ± 0.05	0.117 ± 0.039
[O/Fe]	-0.15	...	-0.22 ^c	-0.12 ^c	-0.13 ^c	-0.17 ^c	-0.16 ± 0.09	-0.11 ± 0.03	-0.146 ± 0.089
[Na/Fe]	0.09	-0.05	0.32	0.23	0.15	0.18	0.22 ± 0.13	0.25 ± 0.06	-0.011 ± 0.032
[Mg/Fe]	-0.29	-0.02	0.14	0.13	0.07	0.17	0.13 ± 0.07	0.27 ± 0.05	-0.003 ± 0.040
[Al/Fe]	0.06	0.09	0.05	0.07	0.07 ± 0.03	0.00 ± 0.03	0.004 ± 0.038
[Si/Fe]	-0.16	-0.06	0.06	0.07	0.02	0.05	0.05 ± 0.04	0.06 ± 0.02	-0.005 ± 0.031
[Ca/Fe]	-0.55	-0.05	0.03	-0.03	0.01	0.03	0.01 ± 0.05	-0.08 ± 0.02	-0.006 ± 0.049
[Sc/Fe]	-1.97	-0.07	0.08	0.02	0.09	0.07	0.06 ± 0.05	-0.04 ± 0.05	0.036 ± 0.024
[Ti/Fe]	0.04	-0.06	-0.10	-0.07	-0.08	-0.04	-0.07 ± 0.04	-0.07 ± 0.03	-0.033 ± 0.059
[V/Fe]	0.03	0.01	0.03	0.02	0.02 ± 0.02	0.06 ± 0.03	0.037 ± 0.036
[Cr/Fe]	0.12	-0.04	0.03	-0.01	0.02	0.04	0.02 ± 0.04	0.05 ± 0.01	0.003 ± 0.031
[Co/Fe]	...	0.00	0.04	0.03	0.09	0.05	0.05 ± 0.05	0.04 ± 0.02	...
[Ni/Fe]	0.47	0.04	0.05	-0.03	0.04	0.04	0.03 ± 0.06	0.02 ± 0.02	-0.028 ± 0.027
[Y/Fe]	0.67	...	-0.01	-0.07	0.04	-0.04	-0.02 ± 0.08	-0.11 ± 0.01	0.007 ± 0.077
[Zr/Fe]	0.01	0.01	0.00	0.05	0.02 ± 0.04
[Ba/Fe]	1.10	0.14	0.27	0.21	0.24	0.29	0.25 ± 0.06	0.33 ± 0.05	0.112 ± 0.035
[La/Fe]	0.03	0.03	0.04	-0.03	0.02 ± 0.06	-0.05 ± 0.02	...

Notes.

^a Carrera & Pancino (2011).

^b Boesgaard et al. (2013).

^c NLTE correction.

lines, of HD 73174 at some phase. Given that the [Fe/H] value shows a large difference between our work and Fossati et al. (2007), we will only compare our results with those of Hui-Bon-Hoa & Alecian (1998) and Burkhart & Coupry (1998) in the following analysis.

Figure 3 shows the comparison of our abundance ratios with results from Hui-Bon-Hoa & Alecian (1998) and Burkhart & Coupry (1998). Most elements have consistent values among the three works except for a slight deviation in the Ni element. Our [Ni/Fe] is slightly higher than the values derived by Hui-Bon-Hoa & Alecian (1998) and Burkhart & Coupry (1998) due to the usage of different lines and log gf values. Hui-Bon-Hoa & Alecian (1998) used only one Ni I line at 5578.75 Å and Burkhart & Coupry (1998) used two lines at 6635.14 and 6643.64 Å, which are included in our line list of ~20 Ni I lines. The log gf values of 6635.14 Å and 6643.64 Å used in Burkhart & Coupry (1998) are about 0.2 lower than ours, and thus their [Ni/Fe] is 0.23 dex lower than ours. In addition, we note that their works did not rescale the abundance to the Sun, and thus our value could be more reliable for this element.

Specifically, HD 73174 has an overabundant [Fe/H] around +0.37 dex, which is 0.2 dex higher than the average value from our four giant stars. Similarly, the Fe-peak element Ni shows a strong overabundance while Cr is slightly enhanced in the present work. Meanwhile, strong underabundances of Ca and Sc in the present work show good agreement with results given by Hui-Bon-Hoa & Alecian (1998) and Burkhart & Coupry (1998). The enhanced Fe, Ni and deficient Ca, Sc are typical characteristics of Am stars, and they are qualitatively explained with diffusion models (e.g., Michaud et al. 1976; Alecian 1996). In this work, as compared with the Sun, s-process elements Y and Ba are clearly overabundant by 1.10 dex and 0.67 dex, respectively. Meanwhile, Burkhart & Coupry (1998) found that the r-process element Eu was also largely overabundant with an [Eu/Fe] value of 0.68 dex. In view of this, we

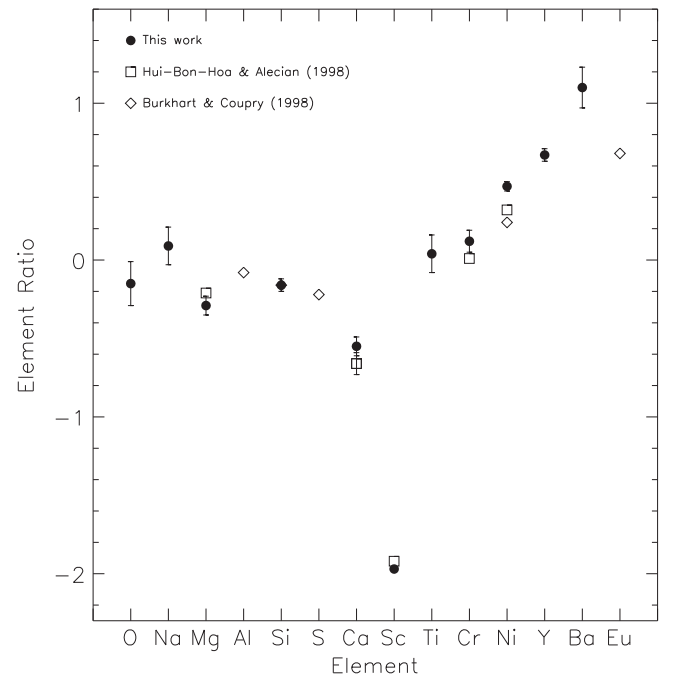


Figure 3. Abundance ratios of HD 73174 from our work (filled circles) compared with the results of Hui-Bon-Hoa & Alecian (1998; open squares) and Burkhart & Coupry (1998; open diamonds).

may suggest that neutron-capture elements are all enhanced in Am stars. Finally, our abundance ratios of O, Mg, and Si are underabundant while the remaining elements, Na and probably Ti, have solar abundance.

5.2. Abundance of the F Dwarf

We have five normal member stars, one F dwarf and four GK giant stars, that have enough lines for abundance

measurements. For the F dwarf, HD 73081, its $[\text{Fe}/\text{H}]$ is lower than the average value of our four GK giant stars, but it is compatible with the result of Boesgaard et al. (2013), who derived $[\text{Fe}/\text{H}]$ values ranging from 0.048 to 0.172 dex for 11 solar-type stars in NGC 2632. We note that the four stars with $[\text{Fe}/\text{H}]$ values lower than 0.1 dex in the sample of Boesgaard et al. (2013) are actually F dwarfs according to Kraus & Hillenbrand (2007). The average metallicity of these four F dwarfs is 0.076 dex which is in agreement with that of HD 73081. Excluding the four F dwarf stars, the average metallicity is 0.140 dex based on the remaining seven G dwarf stars in Boesgaard et al. (2013), which is consistent with our values of GK giant stars but higher than that of F dwarf stars. It seems that F dwarf stars show lower $[\text{Fe}/\text{H}]$ than that of G dwarf and giant stars. This discrepancy appears to be mostly due to our differential abundance analysis relative to the Sun. Since the Sun is a G-type star, we suggest that our abundance results for G-type member stars is more precise and could better represent the true cluster average than F stars.

Our abundance ratios of Na, Mg, Si, Ca, Ti, Cr, Ni, and Ba for HD 73081 are consistent with the values of FG dwarf stars in Boesgaard et al. (2013). Although there is a tendency of lower $[\text{Sc}/\text{Fe}]$ (-0.07) in our work than in that of Boesgaard et al. (2013; from 0.00 to 0.07 dex), the uncertainty of 0.09 dex in our work indicates that it is consistent within errors. According to Uesugi & Fukuda (1970), HD 73081 has a medium rotational velocity of 40 km s^{-1} , which makes the uncertainty of weak lines quite large, and some elements do not have good quality lines for abundance determination. Based on our values and those provided by Boesgaard et al. (2013), there is no clear discrepancy on $[\text{X}/\text{Fe}]$ between F and G dwarf stars.

5.3. Abundances of GK Giant Stars

In our four GK giant stars, three of them (HD 73598, HD 73665, and HD 73710) have been studied by Carrera & Pancino (2011). For comparison, we present the average values of our four giant stars in Column 8, Carrera & Pancino's (2011) three giant stars in Column 9, and Boesgaard et al.'s (2013) 11 solar-type stars in Column 10 of Table 4.

For giant stars, both our work and Carrera & Pancino (2011) give exactly the same $[\text{Fe}/\text{H}]$ of 0.16 dex and very similar abundance ratios of $[\text{X}/\text{Fe}]$ for most elements except for Mg and Y. Our average $[\text{Mg}/\text{Fe}]$ ratio from four giants is 0.13 ± 0.02 , while Carrera & Pancino (2011) gave an average $[\text{Mg}/\text{Fe}] = 0.27 \pm 0.05$ from three giants. The deviation of 0.14 dex is much higher than the analysis uncertainty. This difference mainly results from different atomic data used in these two works. We rescale the $\log gf$ values of Mg lines according to solar abundance based on the moon spectrum, while Carrera & Pancino (2011) chose the VALD reference atomic data. Our differential analysis of stars to the Sun is supported by the consistent $[\text{Mg}/\text{Fe}]$ values between our F dwarf star and 11 solar-type stars provided by Boesgaard et al. (2013). For the Y element, Carrera & Pancino (2011) found $[\text{Y}/\text{Fe}] = -0.11 \pm 0.01$, which appears to be underabundant. However, their uncertainty of $[\text{Y}/\text{Fe}]$ for an individual star is as large as 0.10 dex. In view of this, we may suggest that their $[\text{Y}/\text{Fe}]$ is also compatible with solar, as found in our work.

In both works, Na, Mg, and Ba elements in giant stars show significant enhancements, while $[\text{O}/\text{Fe}]$ is underabundant. It is interesting to investigate the differences in elemental abundances between dwarf and giant stars in the cluster. In this

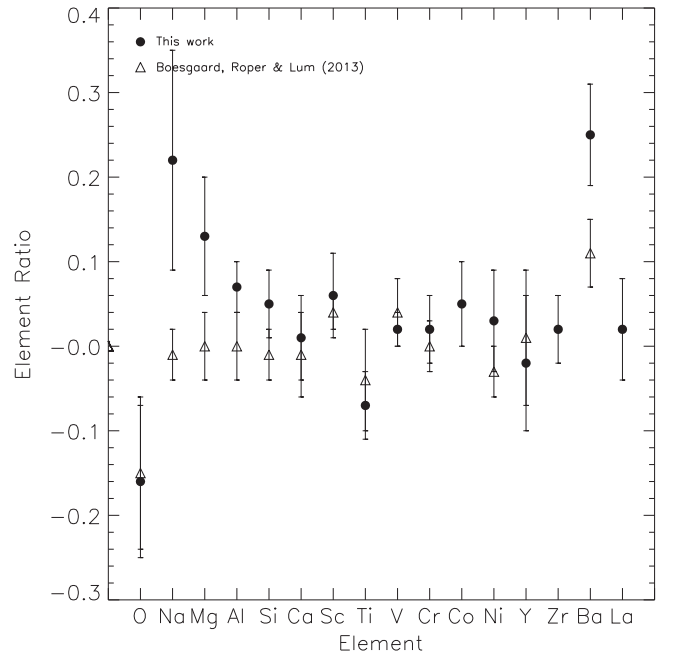


Figure 4. Comparison of abundances between dwarfs and giants. The symbols denote the following: filled circles, average abundance ratios of four giants in this work; open triangles, average abundance ratios of 11 solar-type stars in Boesgaard et al. (2013).

respect, we have compared our results from four giants with average values of 11 solar-type stars from Boesgaard et al. (2013). We have no stars in common with Boesgaard et al. (2013), and thus we cannot rule out the possible systematic differences between our abundance scales and those of Boesgaard et al. (2013). However, we note that Boesgaard et al. (2013) also took moon spectra and normalized their elemental abundances to their lunar/solar values. Thus, our abundances could be approximately on the same scale as Boesgaard et al. (2013). As can be seen from Figure 4, most chemical elements show similar abundance values between dwarfs and giants except for Na, Mg, and Ba elements. The deviations of $\langle[\text{Na}/\text{Fe}]\rangle$, $\langle[\text{Mg}/\text{Fe}]\rangle$, and $\langle[\text{Ba}/\text{Fe}]\rangle$ are 0.23, 0.13, and 0.14 dex, respectively. Since these giants are probably red clump stars according to their locations in the color–magnitude diagram, we can expect that they have undergone somewhat evolutionary effects. The Na enhancement could be a result of the Ne–Na cycle from deeper layers being dredged to the atmospheres of the red giants (Ventura et al. 2001). The increase in Mg in the giants might be due to an increase in ^{26}Mg (Boesgaard et al. 2013). The enhancement of Ba could be on account of the giant stars beginning the AGB stage where Ba can be made by the main s-process (Busso et al. 1999). Finally, to our interests, both dwarfs and giants in NGC 2632 tend to exhibit Ba overabundance and O underabundance with respect to the Sun. This Ba overabundance could be due to the young age (~ 0.7 Gyr) of NGC 2632, according to D’Orazi et al. (2009) who found that $[\text{Ba}/\text{Fe}]$ increased in OCs with younger ages. We suspect that the underabundance of O also results from the young age of NGC 2632.

5.4. Na and O Abundances

We note that $[\text{Na}/\text{Fe}]$ ratios show a large scatter among our four giant stars. In order to investigate if the Na variation is

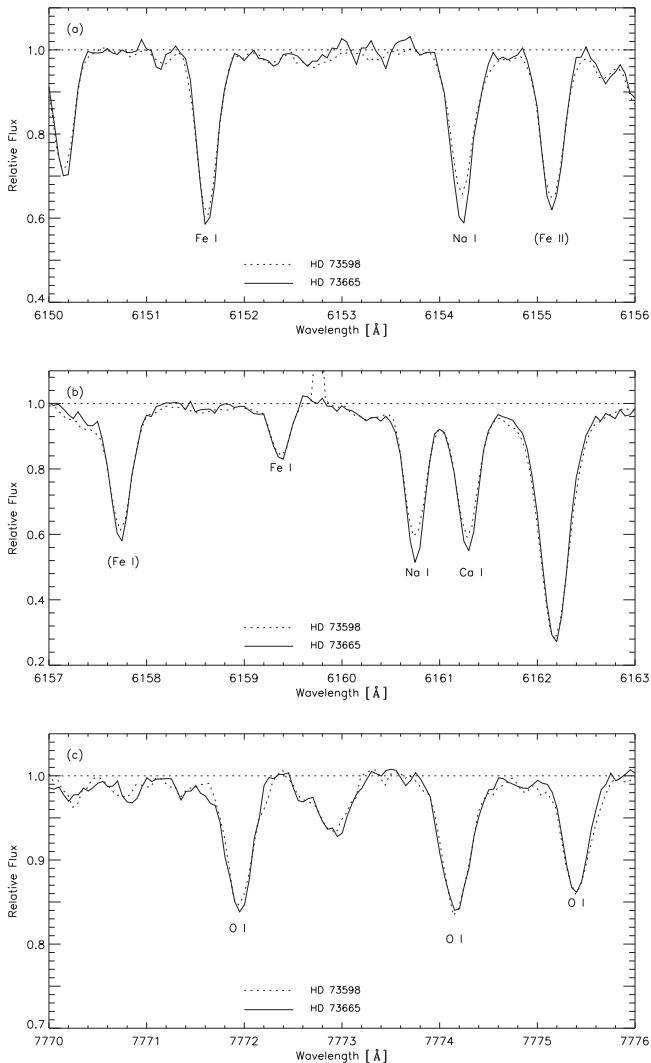


Figure 5. Spectra surrounding two Na I lines (6154.230 and 6160.753 Å) and the O I triplet lines for HD 73598 ($T_{\text{eff}} = 5002$, $\log g = 2.81$, $[\text{Fe}/\text{H}] = 0.16$, $\varepsilon_r = 1.54$) and HD 73665 ($T_{\text{eff}} = 4964$, $\log g = 2.65$, $[\text{Fe}/\text{H}] = 0.20$, $\varepsilon_r = 1.64$). Lines indicated with additional parentheses are blended and not adopted to derive abundances in this work.

real, Figure 5(a) and (b) show spectra surrounding two Na I lines (6154.230 and 6160.753 Å) for two stars with the largest deviation in Na abundance. We can see that the two stars have similar Fe absorption strengths but clear differences in Na absorption strengths, which indicates the existence of differences in $[\text{Na}/\text{Fe}]$ ratios between these two stars. It is noted that HD 73598 is a double or multiple star, but its Na abundance is not affected by its companion in view of consistent abundances of other elements between this star and other member stars. Moreover, differences in absorption strengths for the two Na lines still persist as we compare the spectra between two single stars, HD 73665 and HD 73710. We may suggest that our four giant stars in NGC 2632 show a star-to-star scatter for $[\text{Na}/\text{Fe}]$ ratios.

In view of the dispute on whether there is a Na–O anticorrelation in the OC NGC 6791 (see, e.g., Geisler et al. 2012; Bragaglia et al. 2014; Boesgaard et al. 2015), it is interesting to investigate whether the sodium abundance scattered among Praesepe giants has some relation with such an

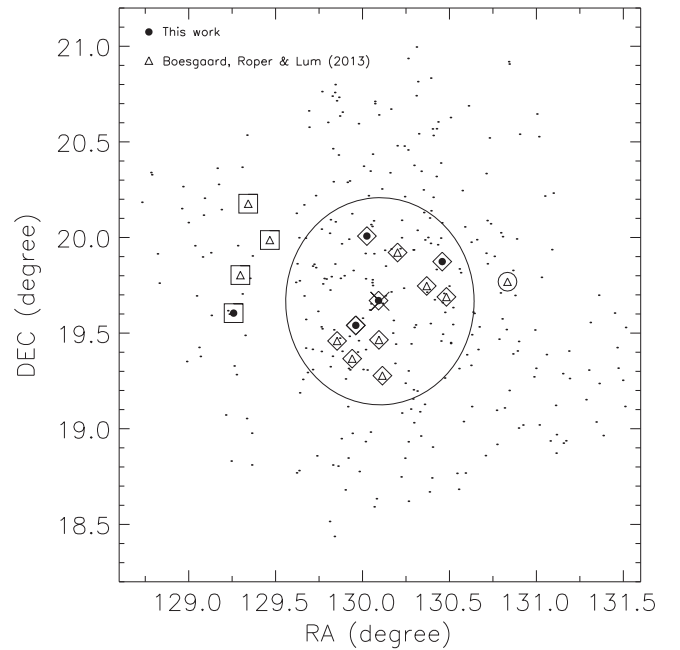


Figure 6. Galactic locations of the 16 stars (open circles and triangles). Different symbols correspond to specific stars: 11 solar-type member stars in Vereshchagin & Chupina (2013; open triangles); five normal stars in our work (filled circles); the cluster center (cross); the core region with a diameter of $65'$ in Vereshchagin & Chupina (2013; solid line); stars in clump 1, clump 2, and clump 3 are marked by additional diamonds, squares, and a circle, respectively.

anticorrelation. We find that the $[\text{O}/\text{Fe}]$ coverage in four giants is only 0.10 dex, which is smaller than the typical error of 0.128 dex (in Table 3). In addition, two stars have almost identical absorption strengths at the O I triplet as shown in Figure 5(c). Small variations in $[\text{O}/\text{Fe}]$ could be caused by different atmospheric parameters. So, there are no convincing differences in O abundances and no evidence for the Na–O anticorrelation in NGC 2632.

In contrast to the Na variation, no significant abundance differences are found for the Mg, Al, and O elements, and these four stars also show consistent C ratios according to Gilroy (1989). Given the present observational uncertainties, it is difficult to either confirm or exclude the small chemical anomaly for the Na element in OC.

5.5. The Connection of Abundance with Spatial Structure

Several studies of the internal structure and kinematics of NGC 2632 indicate that NGC 2632 is an inhomogeneous structure. Vereshchagin & Chupina (2013) suggest that NGC 2632 consists of a homogeneous core and a non-uniform corona. It is interesting to probe whether NGC 2632 will show some hints of inhomogeneous features in abundance. For this purpose, we compile our results with those of 11 solar-type member stars in Boesgaard et al. (2013) to study whether stellar abundances are connected with the spatial structure of NGC 2632. Most of their element abundance values are compatible with our results, except for Na, Mg, and Ba elements which will not be considered in this investigation.

Figure 6 shows the Galactic locations of the total 16 stars, 5 from our work and 11 from Boesgaard et al. (2013). We divide them into three parts, including a central part of the cluster and two clumps in its corona. Table 5 lists the abundance values of these three clumps of stars. For 11 stars in the core region

Table 5
Abundances for Three Clumps of Stars

Ratio	Clump 1											Clump 2				Clump 3
	KW 181	KW 208	KW 212 ^a	KW 253 ^a	KW 283 ^a	KW 288	KW 301	KW 335	KW 399	KW 428 ^a	KW 432	KW 16 ^a	KW 23	KW 30	KW 58	KW 508
[Fe/H]	0.145	0.097	0.16	0.20	0.13	0.080	0.163	0.134	0.077	0.13	0.172	0.06	0.144	0.116	0.109	0.048
[O/Fe]	-0.01	-0.18	-0.13	-0.22	-0.12	-0.13	-0.18	-0.14	-0.23	-0.17	-0.28	...	-0.19	-0.10	-0.19	0.02
[Na/Fe]	-0.01	-0.03	0.15	0.32	0.23	0.03	0.01	-0.01	0.00	0.18	0.00	-0.05	-0.05	-0.06	-0.04	0.04
[Mg/Fe]	-0.07	-0.03	0.07	0.14	0.13	0.04	0.01	0.02	0.02	0.17	-0.01	-0.02	-0.04	-0.02	-0.02	0.07
[Al/Fe]	0.05	-0.02	0.05	0.06	0.09	0.04	-0.07	-0.01	0.01	0.07	0.01	...	-0.01	-0.03	0.01	0.06
[Si/Fe]	-0.04	0.03	0.02	0.06	0.07	0.02	-0.02	0.01	0.01	0.05	-0.04	-0.06	-0.04	-0.02	-0.01	0.05
[Ca/Fe]	-0.01	-0.06	0.01	0.03	-0.03	-0.02	0.00	0.04	-0.01	0.03	0.06	-0.05	0.06	0.00	0.01	-0.04
[Sc/Fe]	0.01	0.04	0.09	0.08	0.02	0.03	0.07	0.00	0.03	0.07	0.07	-0.07	0.05	0.03	0.01	0.06
[Ti/Fe]	-0.06	-0.11	-0.08	-0.10	-0.07	-0.08	-0.06	-0.04	-0.07	-0.04	0.10	-0.06	-0.03	0.02	0.02	-0.05
[V/Fe]	0.04	0.06	0.03	0.03	0.01	0.11	0.02	0.07	0.04	0.02	0.05	...	-0.01	0.03	0.02	-0.02
[Cr/Fe]	0.06	0.02	0.02	0.03	-0.01	0.00	-0.03	0.00	0.01	0.04	0.04	-0.04	0.01	-0.01	-0.02	-0.05
[Ni/Fe]	-0.07	-0.03	0.04	0.05	-0.03	-0.03	0.01	-0.02	-0.05	0.04	0.01	0.04	-0.01	-0.05	-0.01	-0.06
[Y/Fe]	-0.07	-0.11	0.04	-0.01	-0.07	-0.08	0.05	-0.01	-0.01	-0.04	0.00	...	0.15	0.08	0.06	0.01
[Ba/Fe]	0.10	0.08	0.24	0.27	0.21	0.05	0.18	0.14	0.08	0.29	0.13	0.14	0.13	0.13	0.10	0.11

Note.

^a Five normal stars in this work. Other stars are taken from Boesgaard et al. (2013).

(clump 1), their [Fe/H] values show a range from 0.077 to 0.200 dex. Note that, as mentioned in Section 5.2, F dwarf stars seem to show lower [Fe/H] than that of G dwarf and giant stars. Separately, three F dwarfs, KW 208, KW 288, and KW 399, show similar [Fe/H] values and other stars also show consistent metallicities. For other elements, most stars display similar abundance values except that KW 181 shows slightly higher [O/Fe] than other stars and KW 432 shows slightly overabundant [Ti/Fe]. Considering the analysis errors, stars in clump 1 can be suggested to be homogeneous in abundance. We assign four stars, KW 16, KW 23, KW 30, and KW 58, as clump 2. Their abundance ratios are consistent with the values of clump 1 with the exception of [Y/Fe], which shows slightly higher values than the stars of clump 1. We temporarily classify only the star KW 508 as a member of clump 3. We note that KW 508 shows the lowest [Fe/H] and the highest [O/Fe] among these member stars. It is a pity that we have no other stars in the field to confirm this speciality.

Based on the above comparison, there might be some differences (~ 0.1 dex) among member stars for some elements. However, the uncertainties of the abundances also come to about 0.1 dex, which makes us not sure whether these differences are real. At present, we may suggest that there is no significant differences in abundance among stars at different locations of NGC 2632 based on our limited sample and precision.

6. CONCLUSION

We have obtained high-resolution, high S/N spectra for a sample of 18 stars in the field of the OC NGC 2632 with the 2.16 m telescope at Xinglong station of NAOC. Radial velocities for observed stars are obtained from the spectra and used to determine their memberships. Due to large rotational velocities, we have only derived stellar parameters and abundance ratios of 17 elements for one Am star, one F dwarf, and four GK giant stars in our sample. Abundances were obtained in the LTE approximation for all elements, but an NLTE correction was applied for the O element as suggested by Takeda (2003). We have derived an average [Fe/H] value of 0.16 ± 0.06 for NGC 2632 from four giant member stars. As compared with dwarfs, obvious overabundances are found for Na, Mg, and Ba elements in our four giants. Overabundances for Na and Mg in giants can be explained by the evolutionary effect, while two mechanisms, n-capture-enriched Ba in the giants and the young age of NGC 2632, are proposed to explain the Ba enhancement.

There is a star-to-star scatter of [Na/Fe] ratios among our four giant stars but no convincing evidence for the presence of Na–O anticorrelation. Finally, we combined our abundances of five normal member stars with those of 11 solar-type stars from Boesgaard et al. (2013) and divided them into three groups to study whether NGC 2632 will show some hints of an inhomogeneous feature in abundance. However, we do not detect any significant difference in abundance among different groups of stars based on our limited sample; more data are desirable to probe the possible connection between abundance and spatial structure of NGC 2632.

We thank Dr. J. R. Shi for providing the IDL programs for reducing spectra. This study is supported by the National Key Basic Research Program of China (973 program) No. 2014CB845700, the Strategic Priority Research Program of the Chinese Academy of Sciences grant No. XDB01020300, and the National Natural Science Foundation of China under grant Nos. 11390371, 11573035, 1111222326, and 11233004.

REFERENCES

- Adams, J. D., Stauffer, J. R., Skrutskie, M. F., et al. 2002, *AJ*, 124, 1570
- Alecian, G. 1996, *A&A*, 310, 872
- Alonso, A., Arribas, S., & Martínez-Roger, C. 1996, *A&A*, 313, 873
- Alonso, A., Arribas, S., & Martínez-Roger, C. 1999, *A&AS*, 140, 261
- Alonso, A., Arribas, S., & Martínez-Roger, C. 2001, *A&A*, 376, 1039
- Bidelman, W. P. 1956, *PASP*, 68, 318
- Boesgaard, A. M., Lum, M. G., & Deliyannis, C. P. 2015, *ApJ*, 799, 202
- Boesgaard, A. M., Roper, B. W., & Lum, M. G. 2013, *ApJ*, 775, 58
- Boudreault, S., Bailer-Jones, C. A. L., Goldman, B., Henning, T., & Caballero, J. A. 2010, *A&A*, 510, 27
- Bragaglia, A., Sneden, C., Carretta, E., et al. 2014, *ApJ*, 796, 68
- Breger, M., Hareter, M., Endl, M., et al. 2012, *AN*, 333, 131
- Burkhart, C., & Coupry, M. F. 1998, *A&A*, 338, 1073
- Busso, M., Gallino, R., & Wasserburg, G. J. 1999, *ARA&A*, 37, 239
- Carrera, R., & Pancino, E. 2011, *A&A*, 535, A30
- Casewell, S. L., Dobbie, P. D., Napiwotzki, R., et al. 2009, *MNRAS*, 395, 1795
- Castelli, F., & Kurucz, R. L. 2004, arXiv:astro-ph/0405087
- Chen, Y. Q., Nissen, P. E., Zhao, G., Zhang, H. W., & Benoni, T. 2000, *A&AS*, 141, 491
- Debernardi, Y., Mermilliod, J.-C., Carquillat, J.-M., & Ginestet, N. 2000, *A&A*, 354, 881
- Dias, W. S., Alessi, B. S., Moitinho, A., & Lepine, J. R. D. 2002, *A&A*, 389, 871
- Dickens, R. J., Kraft, R. P., & Krzeminski, W. 1968, *AJ*, 73, 6
- D’Orazi, V., Magrini, L., Randich, S., et al. 2009, *ApJL*, 693, L31
- Eggleton, P. P., & Tokovinin, A. A. 2008, *MNRAS*, 389, 869
- Fossati, L., Bagnulo, S., Monier, R., et al. 2007, *A&A*, 476, 911
- Fossati, L., Mochacki, S., Landstreet, J., & Weiss, W. 2010, *A&A*, 510, A8
- Franciosini, E., Randich, S., & Pallavicini, R. 2003, *A&A*, 405, 551
- Friel, E. D., & Boesgaard, A. M. 1992, *ApJ*, 387, 170
- Geisler, D., Villanova, S., Carraro, G., et al. 2012, *ApJL*, 756, L40
- Gilroy, K. K. 1989, *ApJ*, 347, 835
- Girardi, L., Bressan, A., Bertelli, G., & Chiosi, C. 2000, *A&AS*, 141, 371
- Holland, K., Jameson, R. F., Hodgkin, S., Davies, M. B., & Pinfield, D. 2000, *MNRAS*, 319, 956
- Hui-Bon-Hoa, A., & Alecian, G. 1998, *A&A*, 332, 224
- Kafka, S., & Honeycutt, R. K. 2006, *AJ*, 132, 1517
- Kraus, A. L., & Hillenbrand, L. A. 2007, *AJ*, 134, 2340
- Kurucz, R. 1993, Kurucz CD-ROM No. 13 (Cambridge, MA: Smithsonian Astrophysical Observatory)
- Liu, F., Chen, Y. Q., Zhao, G., et al. 2012, *MNRAS*, 422, 2969
- Michaud, G., Charland, Y., Vauclair, S., & Vauclair, G. 1976, *ApJ*, 210, 447
- Pace, G., Pasquini, L., & Frano, J. S. P. 2008, *A&A*, 489, 403
- Pourbaix, D., Tokovinin, A. A., Batten, A. H., et al. 2004, *A&A*, 424, 727
- Ramírez, I., Meléndez, J., & Asplund, M. 2014, *A&A*, 561, L7
- Salaris, M., Weiss, A., & Percival, S. M. 2004, *A&A*, 414, 163
- Takeda, Y. 2003, *A&A*, 402, 343
- Taylor, B. J. 2006, *AJ*, 132, 2453
- Tsantaki, M., Sousa, S. G., Adibekyan, V. Zh., et al. 2013, *A&A*, 555, A150
- Uesugi, A., & Fukuda, I. 1970, Catalogue of Rotational Velocities of the Stars (Kyoto: Univ. of Kyoto)
- Ventura, P., D’Antona, F., Mazzitelli, I., & Gratton, R. 2001, *ApJL*, 550, L65
- Vereshchagin, S. V., & Chupina, N. V. 2013, *AN*, 334, 892
- Wang, P. F., Chen, W. P., Lin, C. C., et al. 2014, *ApJ*, 784, 57
- Yi, S. K., Kim, Y.-C., & Demarque, P. 2003, *ApJS*, 144, 259